

Research Article

Near-Ground Path Loss Measurements and Modeling for Wireless Sensor Networks at 2.4 GHz

Daihua Wang,¹ Linli Song,² Xiangshan Kong,³ and Zhijie Zhang¹

¹ National Key Laboratory for Electronic Measurement Technology, North University of China, Taiyuan 030051, China

² Key Laboratory of Instrumentation Science and Dynamic Measurement of The Ministry of Education, North University of China, Taiyuan 030051, China

³ North Automatic Control Technology Institute, CNGC, Taiyuan 030006, China

Correspondence should be addressed to Daihua Wang, hdwang_2008@yahoo.com.cn

Received 25 March 2012; Revised 18 June 2012; Accepted 29 June 2012

Academic Editor: George P. Efthymoglou

Copyright © 2012 Daihua Wang et al. This is an open access article distributed under the Creative Commons Attribution License, which permits unrestricted use, distribution, and reproduction in any medium, provided the original work is properly cited.

Near-ground channel characterization is an important issue in most military applications of wireless sensor networks. However, the channel at the ground level lacks characterization. In this paper, we present a path loss model for three near-ground scenarios. The path loss values for each scenario were captured through extensive measurements, and then a least-square linear regression was performed. This indicates that the log-distance-based model is still suitable for path loss modeling in near-ground scenarios, and the prediction accuracy of the two-slope model is superior to that of the one-slope model. The validity of the proposed model was further verified by comparisons between the predicted and measured far-field path losses. Finally, compared to the generic models, the proposed model is more effective for the path loss prediction in near-ground scenarios.

1. Introduction

Wireless sensor networks (WSNs) are an enabling technology for the distributed monitoring of industrial, military, and natural environments [1, 2]. In most military applications, the sensors are placed at the ground level, and their antennas rise a few centimeters above the ground [3, 4]. However, almost all studies to date were based on the assumption that the antennas were placed one meter or more above the ground, which could not accurately capture the behavior of an authentic WSN [3]. It is well known that the signal strength and associated noises are affected by the channel characteristics, which depend on an authentic testing environment. Therefore, the propagation characteristics of near-ground environments are important to system designers for network planning [5, 6].

The rise of WSN applications has prompted the need for a more complete understanding of near-ground propagation channels. In [7], one of the first studies of near-ground wideband channel measurement was conducted in 800–1000 MHz, and eleven indoor or outdoor sites were measured with an antenna height of approximately 15 cm. In

[8, 9], another two earlier works related to near-ground RF propagation measurement were carried out for military or emergency applications at the frequency of 915 and 879 MHz, respectively. The authors investigated the scenario of a person lying on the ground attempting to place a call with an antenna very near the ground (several or several tens of centimeters in height). Joshi et al. presented narrowband and wideband channel measurement results at 300 and 1900 MHz for near-ground propagation with characterizing the effect of antenna heights, radiation patterns, and foliage environments [10], but the lowest antenna height was 0.75 m, which was insufficient for an authentic near-ground scenario. Martínez-Sala et al. presented the near-ground channel characterization for WSNs in three outdoor scenarios, validated a two-slope lognormal path loss channel model at 868 MHz, and compared it to the widely used one-slope model [3]. Subsequently, Meng et al. investigated near-ground radio wave propagation in a tropical forest in the VHF and UHF (40, 80, 250, and 550 MHz) bands [11]. The antenna height selected in their measurement campaigns was 2.15 m, which was not the expected case for most WSNs when established in outdoor environments. Other research



FIGURE 1: Photograph of the measurement sites.

activities related to near-ground channels included the study of radio wave propagation in a car park at 433 MHz [6] and assessment of indoor or industrial ultrawideband (UWB) channels [4, 5, 12].

As stated above, although attention has recently focused on modeling near-ground propagation channels, few studies investigate propagation in near-ground environments with antenna heights in several centimeters level, especially for the 2.4 GHz band. In this paper, we propose a statistical model for near-ground channels based on extensive measurements.

The initial intention of the work is to assess the coverage capability of a WSN developed for data (pressure or temperature) acquisition in military explosive research. The sensor nodes are fixed on the ground in the explosion field for the testing task, and the antenna height of sensor nodes is set as low as 3 cm to resist physical damage from nearby detonations. It is well known that, due to the proximity of the antenna to the ground, significant performance degradation may occur [3, 4]. So, effective path loss prediction becomes a key issue in system design. In fact, different propagation models should be applied in different environments, but to our knowledge, no appropriate model exists for the near-ground scenario. Therefore, the results of extensive measurements and path loss modeling in the authentic application environment are presented in this paper. For the purposes of comparison, two other representative environments are selected as measurement sites. In all the sites, the same measurement and analysis procedures are applied, and the derived model is validated by far-field measurement data. Finally, the performance of the obtained model is compared with the generic models.

The paper is organized as follows: in Section 2, the scenarios are described in further detail. In Section 3, the measurement methodology is summarized. In Section 4, the measured results and a discussion of each site's results are presented. A path loss model for near-ground radio wave

propagation is derived and then compared with the previous models. The summary and conclusions are presented in Section 5.

2. Near-Ground Scenarios

Generally, the target scenario for outdoor WSN application is just above ground level. Sensor nodes with a very low antenna height are placed on the ground randomly or regularly. Near-ground scenario is a complex environment due to reflection, obstruction, and absorption occurring from the ground and vegetation [6, 10]. Channel measurements and modeling are, therefore, a basic necessity for system design. Three different outdoor environments were selected in this work, including a large plaza, a straight sidewalk, and an open grassland (see photographs in Figure 1).

The first site is located at the school yard of North University of China (NUC). It is a rectangular-shaped site (an area of $115 \times 100 \text{ m}^2$) bordered by trees and several buildings. The trees are almost equally spaced, with a separation of 2 m, and their trunks have a diameter of no more than 10 cm. The ground is paved with bricks, and the terrain is fairly flat. The second site is a straight sidewalk along with suburban road, and the other side is a large plot of lowland with scattered trees. The sidewalk is paved with pitch and bricks, and the terrain is nearly flat. A line of lampposts are spaced 35 m apart along the sidewalk, and several low trees are nearly equally spaced between the lampposts. The lamppost has a conical profile with a maximum diameter of 20 cm at the base, and the dimensions are comparable to the radio wavelength. The open grassland is the authentic application environment for WSN in testing experiments. The terrain is basically flat, consisting of soil and sand. Most of the areas are covered by vegetation, and a large number of shrubs are scattered in the areas with an average height of approximately 40 cm. Given the low antenna height, this environment can be seen as a non-line-of-sight (NLOS) situation.

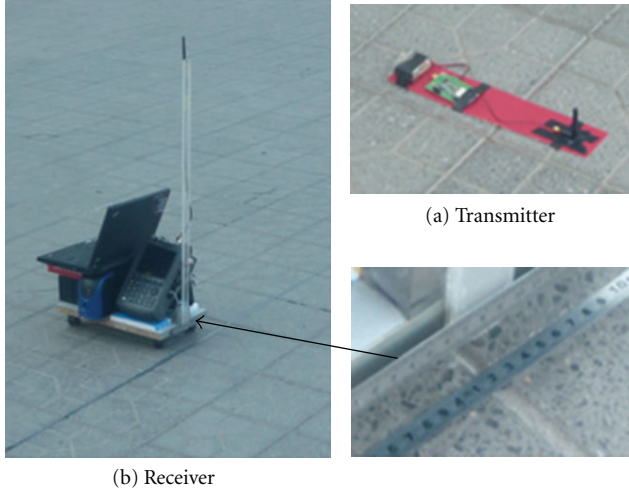


FIGURE 2: Photograph of the measurement setup.

Although the terrain is flat, as can be seen from Figure 1, significant attenuation in radio wave propagation will exist due to the very low antenna height. This is further verified in Section 4. Furthermore, each site has different features and thus can be predicted to have its own exclusive propagation characteristics.

3. Measurement Methodology

For the purpose of conducting an experimental channel characterization for path loss assessment, only narrowband measurement trials were carried out. The sensor node had a narrowband RF transceiver working at 2.4 GHz, which was used as a transmitter. The receiver consisted of a portable spectrum analyzer and a laptop computer illustrated in Figure 2. The spectrum analyzer (Agilent N9912A) acquired signal strength data, and the laptop computer was used for data storage. A pair of vertical-polarization omnidirectional antennas with a calibrated gain of 2 dBi were used as transmitting and receiving antennas. Both antennas were connected to the transmitter or receiver by a low-loss coaxial cable. During the measurements, the transmitter sent a carrier of 19 dBm (maximum radiated power for radio range extension) at 2.4 GHz, and the spectrum analyzer was set to this central frequency.

At each of the three previously mentioned sites, the same methodology was applied. The transmitter was fixed in a position with different antenna heights of 3 cm and 1 m. The receiver was separated from the transmitter by up to 100 m, and the antenna height was varied from 1 to 2 m. Along the straight line followed by the receiver, the samples were collected every meter in a distance of up to 10 meters from the transmitter, and then every 2 meters until the end. At each nominal position, 10 testing points over 10 cm around the central position were selected for spatial averaging, 20 samples were collected at each testing point for time averaging, and 200 samples were acquired in total. In practice, since

the sensor nodes do not move, stationary testing points were selected. In addition, there was no moving machinery at the sites during the measurements, and no moving personnel. Therefore, it is reasonable to assume that the measurement environment is stationary, and the channel of interest is slowly time varying [7]. Special attention was paid to various antenna heights in the measurement because the server node (receiver) has an antenna height of about 1–3 m higher than the sensor nodes in practical applications. Also, to compare performance, an antenna height of 1 m was selected as the same case in the measurements for all the sites.

4. Channel Modeling and Analysis

After data collection, 55 datasets were recorded in one measurement campaign, and the raw data in each dataset was examined firstly to eliminate the singular point. In order to obtain a mean value of the measured signal strength, for a nominal position, time averaging for each testing point around the central position was firstly performed, and then spatial averaging was performed among the testing points, which could mitigate the effects of the small-scale fading. Subsequently, the local mean path loss was calculated. Based on the preliminary analysis, it is found that the path loss tends to a linear relation with the log-distance, so the log-distance-based path loss model can be used for channel characterization. The measured results and the process of modeling are presented in Section 4.1, and the validity of the model is verified with the experimental data in Section 4.2. Two generic models related to the near-ground scenarios are briefly introduced in Section 4.3, and their performances on the path loss prediction are compared with the proposed model.

4.1. Path Loss Modeling. Path loss is a fundamental characteristic of radio wave propagation, which is often used for link budget calculation and determining transceiver ranges [4]. For radio wave propagation in outdoor environments, both theoretical and measurement-based propagation models indicate that the average of received signal power decreases logarithmically with the distance [13, 14]. In this section, the measured path losses versus the log-distance are plotted in Figures 3, 4, and 5 for all the sites, and an approximate linear relation can be found between the path loss and the log-distance. So the linear regression can be used for data fitting, and the process is summarized as follows.

4.1.1. Linear Regression. Assume that there are m samples at the transmitter-receiver (T-R) separation distance of d_1, d_2, \dots, d_m , and the measured values of the path loss are $L(d_1), L(d_2), \dots, L(d_m)$, respectively. The relation between the path loss and the T-R distance can be expressed as follows:

one-slope model:

$$L(d_i) = L(d_0) + 10n \log_{10} \left(\frac{d_i}{d_0} \right) + \varepsilon_i, \quad i = 1, 2, \dots, m, \quad (1)$$

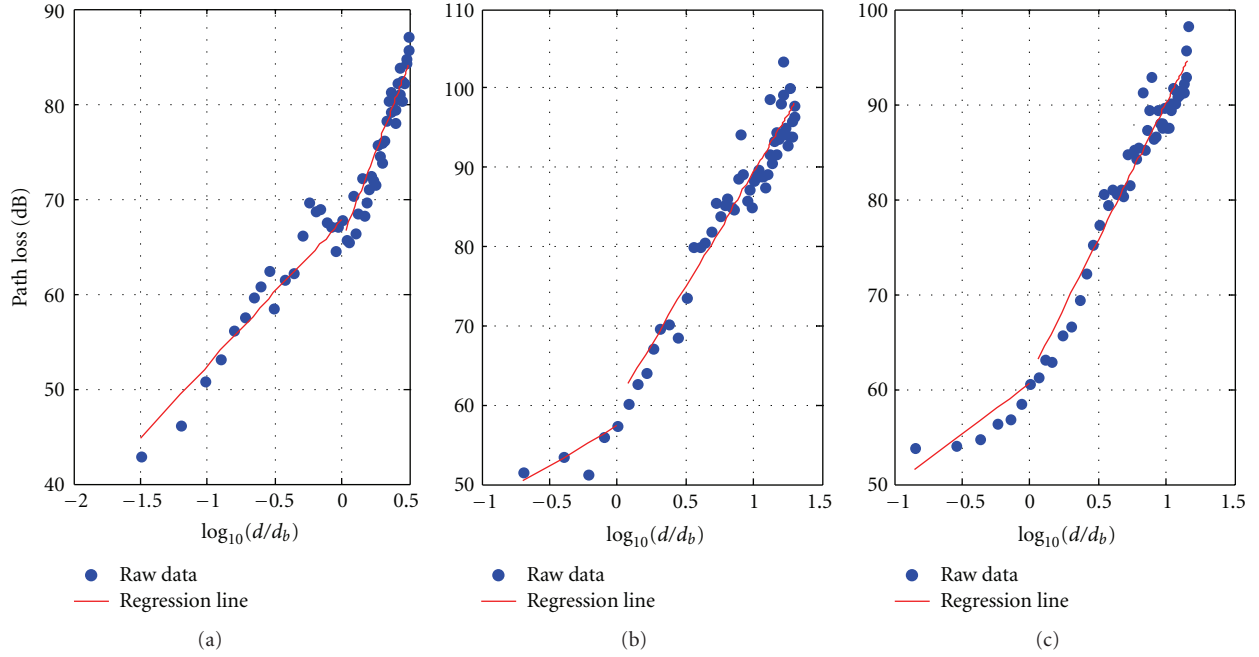


FIGURE 3: The measured path loss and the regression lines in the plaza. (a) $h_t = h_r = 1$ m. (b) $h_t = 3$ cm and $h_r = 1$ m. (c) $h_t = 3$ cm and $h_r = 2$ m.

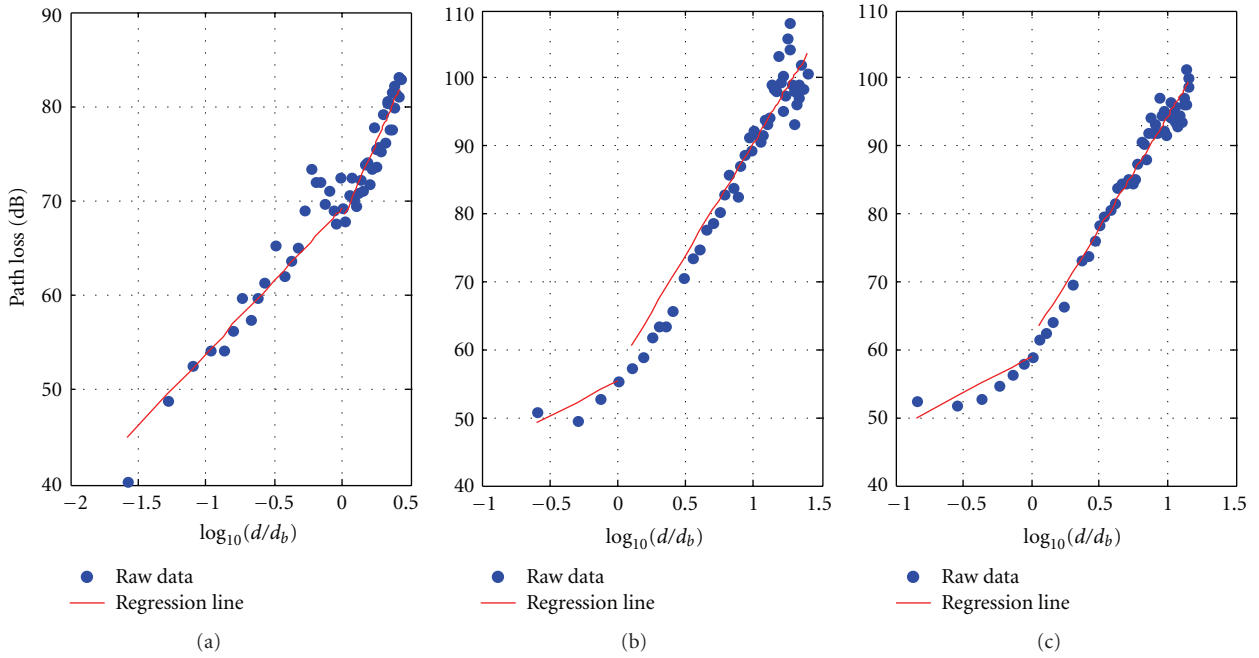


FIGURE 4: The measured path loss and the regression lines in the sidewalk. (a) $h_t = h_r = 1$ m. (b) $h_t = 3$ cm and $h_r = 1$ m. (c) $h_t = 3$ cm and $h_r = 2$ m.

two-slope model:

$$L(d_i) = \begin{cases} L(d_b) + 10n_1 \log_{10}\left(\frac{d_i}{d_b}\right) + \varepsilon_{1i}, & d_i \leq d_b \\ L(d_{b+1}) + 10n_2 \log_{10}\left(\frac{d_i}{d_b}\right) + \varepsilon_{2i}, & d_i > d_b \end{cases} \quad i = 1, 2, \dots, m, \quad (2)$$

where in (1) d_0 is a reference distance close to the transmitter, and $L(d_0)$ is the path loss value at d_0 . In (2), two different slopes are defined before and after a breakpoint d_b which is determined by measurements close to the transmitter. The $L(d_b)$ and $L(d_{b+1})$ are selected as the reference path losses before and after the breakpoint, respectively. For the two models, n , n_1 , and n_2 are the path loss exponents which indicate the attenuation rate; ε_i , ε_{1i} , and ε_{2i} are a set of

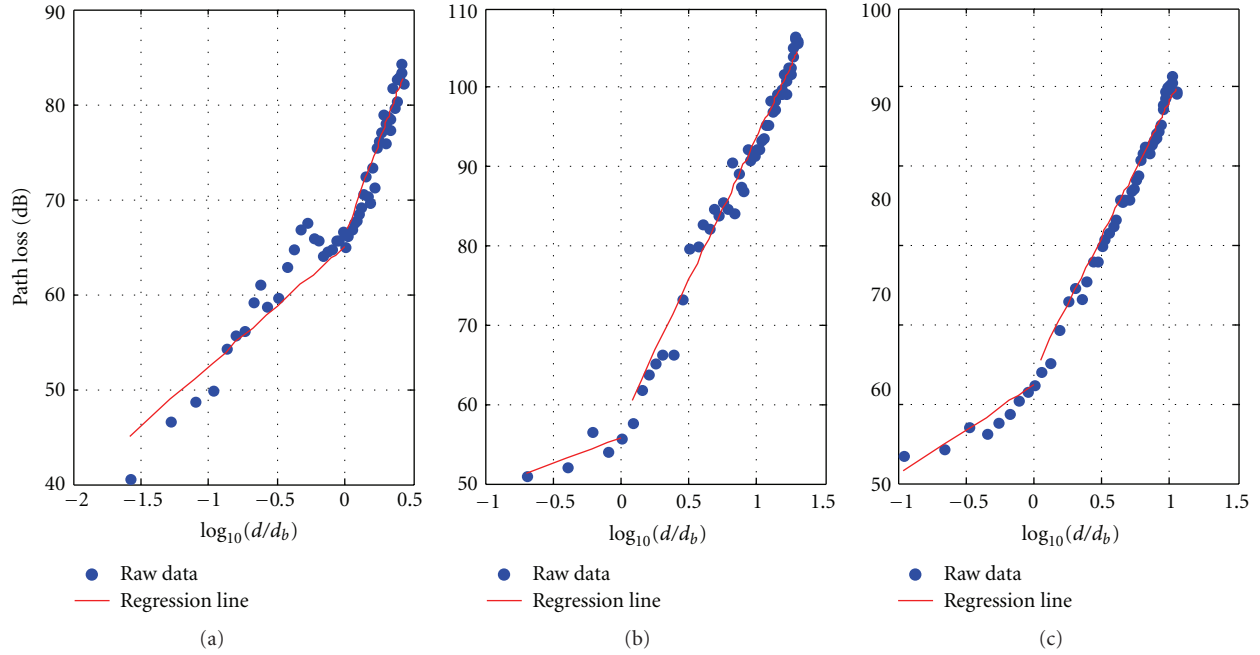


FIGURE 5: The measured path loss and the regression lines in the grassland. (a) $h_t = h_r = 1$ m. (b) $h_t = 3$ cm and $h_r = 1$ m. (c) $h_t = 3$ cm and $h_r = 2$ m.

zero-mean random variables with standard deviation σ , σ_1 , and σ_2 , respectively.

Then, the linear regression can be executed in MATLAB by using the least-square method. Assume that $\hat{L}(d_i)$ is the regression value of the sample $L(d_i)$, then the residual sum of square (RSS) between $L(d_i)$ and $\hat{L}(d_i)$ is defined as (for the two-slope model)

$$\begin{aligned} \mathcal{Q}(b, n_1, n_2) &= \sum_{i=1}^b \left(L(d_i) - L(d_b) - 10n_1 \log_{10} \left(\frac{d_i}{d_b} \right) \right)^2 \\ &+ \sum_{i=b+1}^m \left(L(d_i) - L(d_{b+1}) - 10n_2 \log_{10} \left(\frac{d_i}{d_b} \right) \right)^2. \end{aligned} \quad (3)$$

During the process of regression, the value of $\mathcal{Q}(b, n_1, n_2)$ should be minimized when tuning the parameters b , n_1 and n_2 . Because b is an unknown location of breakpoint, which also has an important effect on determining the slopes of the two-segment regression line, a traversal in sequence from 2 to $m - 1$ is executed to find out the best location of breakpoint for the minimization of $\mathcal{Q}(b, n_1, n_2)$. The process is as follows: firstly, for a certain b , the n_1 and n_2 are obtained by using the least-square method, and the $\mathcal{Q}(b, n_1, n_2)$ is calculated according to (3); secondly, repeat the first step with varied b and a set of $\mathcal{Q}(b, n_1, n_2)$ is created; thirdly, find out the minimum value of $\mathcal{Q}(b, n_1, n_2)$ in its set and then the optimized parameters b , n_1 , and n_2 can be determined.

The regression process of the one-slope model is similar to that of the two-slope model. However, the breakpoint does not need to be calculated, and d_0 in (1) can be directly set to the T-R distance of 1 m.

Finally, in order to examine the goodness of logarithmic fit, two statistical parameters, that is, the residual standard deviation (σ) and the correlation coefficient (R^2), are calculated. The residual standard deviation measures the mean deviation of the measured path losses to the predicted values by using the fitting model. A value of σ closer to 0 indicates a better fit. The parameter is defined as (for the two-slope model)

$$\begin{aligned} \sigma_1 &= \sqrt{\frac{\sum_{i=1}^b (L(d_i) - \hat{L}(d_i))^2}{b - 2}}, \\ \sigma_2 &= \sqrt{\frac{\sum_{i=b+1}^m (L(d_i) - \hat{L}(d_i))^2}{m - b - 2}}, \end{aligned} \quad (4)$$

where $L(d_i)$ is the measured path loss and $\hat{L}(d_i)$ is the predicted path loss, and subscripts 1 and 2 indicate the values before and after the breakpoint, respectively.

The correlation coefficient represents how successful the fit is in explaining the variation of the data. It is defined as the square of the correlation between the measured and the predicted path losses. For the two-slope model, it can be expressed as

$$\begin{aligned} R_1^2 &= 1 - \frac{\sum_{i=1}^b (L(d_i) - \hat{L}(d_i))^2}{\sum_{i=1}^b (L(d_i) - \bar{L}(d_i))^2}, \\ R_2^2 &= 1 - \frac{\sum_{i=b+1}^m (L(d_i) - \hat{L}(d_i))^2}{\sum_{i=b+1}^m (L(d_i) - \bar{L}(d_i))^2}, \end{aligned} \quad (5)$$

TABLE 1: Model parameters for all the sites.

Site	Plaza			Sidewalk			Grassland		
Transmitting antenna height, h_t	1 m	3 cm	3 cm	1 m	3 cm	3 cm	1 m	3 cm	3 cm
Receiving antenna height, h_r	1 m	1 m	2 m	1 m	1 m	2 m	1 m	1 m	2 m
One-slope model									
n	1.86	2.21	1.86	1.99	2.47	2.14	1.90	2.48	2.08
$L(d_0)$ (dB)	42.86	51.51	53.81	40.36	50.91	52.49	40.51	51.08	53.56
σ (dB)	3.25	4.34	4.62	2.45	5.74	5.23	3.02	5.19	5.59
R^2	0.89	0.89	0.86	0.93	0.87	0.87	0.91	0.89	0.85
d_{\max} (m)	6664	680	1711	5117	362	739	7507	346	810
Two-slope model									
n_1	1.52	1.00	1.06	1.55	1.01	1.05	1.26	0.65	1.14
n_2	3.74	2.91	2.87	3.34	3.31	3.29	3.93	3.62	3.43
$L(d_b)$ (dB)	67.68	57.29	60.54	69.29	55.35	58.87	65.03	55.69	62.36
$L(d_{b+1})$ (dB)	65.61	60.26	61.36	67.84	57.36	61.44	66.09	57.57	64.04
σ_1 (dB)	2.49	1.99	1.75	3.09	2.02	1.69	2.98	1.37	1.39
σ_2 (dB)	1.85	2.94	2.25	1.55	3.47	2.01	1.51	1.90	1.42
R_1^2	0.89	0.43	0.50	0.87	0.34	0.64	0.84	0.65	0.80
R_2^2	0.91	0.92	0.94	0.88	0.93	0.96	0.93	0.98	0.98
d_b (m)	32	5	7	38	4	7	38	5	9
d_{\max} (m)	631	351	475	916	205	278	627	182	259
Plane-earth model									
d_{\max} (m)	708	123	173	708	123	173	708	123	173
Free-space model									
d_{\max} (m)					4983				

Where $\bar{L}(d_i)$ is the mean of the measured path losses. The value of R^2 is between 0 and 1; as it reaches 1, the regression curve tends to align more accurately with the raw data.

The calculation of these two statistical parameters for the one-slope model is similar to that above defined with no breakpoint.

4.1.2. Statistical Parameters. The regression line of the path loss is also drawn for each data set in Figures 3–5, and the key parameters for each model are summarized in Table 1. Figures 3–5 illustrate that the regression line tends to a better fit to the raw data for all the sites, which can be further verified by the statistical parameters in Table 1. It is confirmed consistently in Table 1 that for the two-slope model, the residual standard deviation (σ_2) has lower values than that for the one-slope model (σ). In the case of the open grassland, for example, the values of σ_2 are better than σ by 1.51–4.17 dB. Simultaneously, Table 1 shows that the values of R_2^2 in the two-slope model are closer to 1 than those in the one-slope model (R^2). In addition, for the two-slope model, it should be noted in Figures 3–5 that the first segment of the regression line does not fit very well to the raw data, which is a result of the poor values of R_1^2 in Table 1. This is mainly due to the small number data points before the breakpoint; that is, the breakpoint is too close to the transmitter. In the case of $h_t = h_r = 1$ m for all the sites, although the number of data points before the breakpoint is more than in other cases, significant fluctuations occur in the path loss, which cause difficulties for the regression,

illustrated by the poor values of σ_1 and R_1^2 . Nevertheless, for the purpose of path loss prediction, more attention should be focused on investigating signal attenuation in far field. So it can be affirmed that the two-slope model is a better choice for channel characterization in near-ground sites.

4.1.3. Breakpoint Distance. It is observed from Figures 3–5 that there is a certain breakpoint among each data set which indicates different change rate of the path loss, and intuitively, the breakpoint distance varies in different data sets. In general, when a LOS condition is available, the breakpoint distance can be estimated by [15, 16]

$$d_b = \frac{4h_t h_r}{\lambda}. \quad (6)$$

For the three cases, where $h_t = h_r = 1$ m, $h_t = 3$ cm and $h_r = 2$ m, and $h_t = 3$ cm and $h_r = 1$ m, the estimated values of d_b in (6) are 32, 1.92, and 0.96 m, respectively. Compared to the values in Table 1, it is found that there is an obvious difference between the estimated results and the traversal results. This is because the expression in (6) is based on the assumption of $d_b \gg h_t, h_r$, while the condition cannot be reached in the near-ground scenarios. However, the estimated values can be partly used to verify the traversal results. In addition, it can be seen from Table 1 that, for a given antenna height, the breakpoint distances are similar in each site. This indicates that there is a strong link between the breakpoint distance and the antenna height. The slight variations in the breakpoint distance can be attributed to

the influences of different environments. Furthermore, for a certain site, the breakpoint distance varies depending on the antenna height. As the antenna height decreases, the breakpoint moves closer to the transmitter. This is because a bigger Fresnel zone is intercepted by the ground (with the covered vegetation) when the antenna height is lower. So, it can be concluded that the breakpoint distance is mainly determined by the antenna height with slight environmental effects.

4.1.4. Path Loss Exponent. The resulting values of the path loss exponent are also given in Table 1. It is found that, for the one-slope model, the n value is around 2 and varies between 1.86 and 2.48, which corresponds to 18.6–24.8 dB attenuation per decade of distance. Intuitively, this attenuation rate seems low, even compared to the free-space model ($n = 2$). In the case of the sidewalk, where $h_t = h_r = 1$ m, for example, the n value of 1.99 is almost the same as the n value in the free-space model. However, it is obvious that the authentic environment of the sidewalk (with a low antenna height) is far from a free space. That is, the one-slope model will induce large errors in the path loss prediction, which is further confirmed in Section 4.2.

For the two-slope model, Table 1 illustrates that the slope before the breakpoint (n_1) is less than 2, while the slope after the breakpoint (n_2) is between 2 and 4, which corresponds to the results obtained in [17]. In the case of $h_t = 3$ cm ($h_r = 1$ or 2 m) for all the sites, the relatively small values of n_1 are mostly due to the fact that there are fewer data points before the breakpoint, and data fluctuation thus has a strong influence on the n_1 value. After the breakpoint, for a given antenna height, the n_2 value for the grassland is larger than that for the sidewalk, and the latter is larger than that for the plaza. This is in accordance with the authentic environment. The only exception is that the n_2 value for the sidewalk is less than that for the plaza when $h_t = h_r = 1$ m. This may be due to the extra multipath components caused by the unique surroundings of the plaza, such as buildings and big trees. When both the antenna heights are set to 1 meter, the Fresnel zones are not easily obstructed by the ground (this can be verified by the larger distance of breakpoint), which implies that more energy will be radiated directly onto the surroundings and therefore induce more multipath components among the radio wave signals. As the transmitting antenna height decreases, this propagation mechanism in the plaza is mitigated, and the path loss is relatively weaker. As can be seen from Figures 7 and 8, in the other two cases of lower transmitting antenna heights, the path loss for the sidewalk is larger than that for the plaza by 7.3–7.9 dB at a 400 m distance.

Another phenomenon that should be mentioned is that although the n_2 value for the grassland is larger than for the plaza when $h_t = h_r = 1$ m, the initial part of the path loss for the grassland is still less than for the plaza. This is mainly due to the fact that the breakpoint distance for the plaza is closer to the transmitter than for the grassland. As the T-R distance increases, the path loss occurs at much closer ranges compared to each other. And after the T-R distance of 600 m,

the path loss for the grassland becomes larger than for the plaza.

From Figures 7 and 8, the path loss for the grassland is closer to that of the sidewalk, which seems not to fit well with the authentic environment. This is not surprising, since at 2.4 GHz frequency, the wavelength of the signal is comparable in size with the dimensions of the vegetation. Hence, more forward scattering is caused by the dense vegetation. This forward scattering can counteract the loss due to absorption and attenuation caused by the vegetation, thus the much lower attenuation rate [11]. Moreover, in Figure 7, the difference in path loss between the two sites is further reduced as the h_r value increases to 2 m. This is because the transmission distance through the vegetation is decreased while increasing the receiving antenna height, which results in a lower path loss for the grassland.

In addition, for a given site, the path loss when $h_t = 3$ cm and $h_r = 1$ m is larger than when $h_t = 3$ cm and $h_r = 2$ m, and the latter is larger than that when $h_t = h_r = 1$ m. For the sites of the sidewalk and the grassland, when the receiving antenna is fixed at a height of 1 m, the path loss increases by 20.1–21.97 dB as the transmitting antenna height is decreased from 1 m to 3 cm; when the transmitting antenna is fixed at a height of 3 cm, an increase of 4.31–5.9 dB in the path loss is observed as the receiving antenna height is decreased from 2 to 1 m.

4.2. Verification with the Measured Data. To prove the validity of the proposed model, for the sites of sidewalk and grassland, the path loss for different locations far from the transmitter was measured and then compared with the value predicted by the proposed model. The plaza site was not further measured due to the restriction of area, and the verification could not be carried out. Several typical testing points for the other two sites are presented in Tables 2 and 3, where PL is the measured path loss at a T-R distance d ($\gg d_b$); Δ_1 and Δ_2 are the difference between the PL value and the predicted value by the one-slope model and the two-slope model, respectively. It is found that the predicted values by the two-slope model are in good agreement with the measured values. The absolute value of the difference Δ_2 is 0.28–6.66 dB, and most of them are less than 3 dB. For the one-slope model, the difference Δ_1 is 5.17–20.45 dB, which indicates poor prediction accuracy. This can be further verified by the d_{\max} value in Table 1. The maximum transmission distance of d_{\max} is calculated for a transmitted power of 19 dBm and a sensitivity of –95 dBm for all the models. As can be seen from Table 1, the d_{\max} value for the one-slope model is about 2–12 times that for the two-slope model. Therefore, it is concluded that, for the path loss prediction, the two-slope model is more restrictive than the one-slope model.

4.3. Comparison to the Generic Models. In order to provide a better representation of the proposed model, the performance of the two-slope model is compared with that of the generic models. Due to the flat terrain at all three sites, the free-space model can be compared with the two-slope model.

TABLE 2: Comparisons between the predicted path loss and the measured path loss in far field for the sidewalk.

h_t versus h_r	1 m versus 1 m			3 cm versus 1 m			3 cm versus 2 m		
d (m)	150	400	700	150	180	200	150	200	250
PL (dB)	88.83	102.49	112.07	112.13	114.07	113.88	111.89	110.91	113.63
Δ_1 (dB)	5.17	10.35	15.09	7.47	7.45	6.13	12.83	9.18	9.82
Δ_2 (dB)	1.07	0.51	1.97	2.67	1.99	0.28	6.66	1.57	1.10

TABLE 3: Comparisons between the predicted path loss and the measured path loss in far field for the grassland.

h_t versus h_r	1 m versus 1 m			3 cm versus 1 m			3 cm versus 2 m		
d (m)	200	400	600	150	180	200	150	180	200
PL (dB)	90.99	108.41	113.74	113.04	112.83	114.92	108.46	109.81	112.21
Δ_1 (dB)	6.76	18.46	20.45	7.99	5.82	6.77	9.64	9.34	10.79
Δ_2 (dB)	-3.44	2.14	0.55	2.00	-1.08	-0.64	2.51	1.14	1.98

The path loss for the free-space model [18] at 2.4 GHz is given as

$$L_{FS} = 100 + 20 \log_{10}(d), \quad (7)$$

where d is the distance between the transmitter and receiver in kilometers.

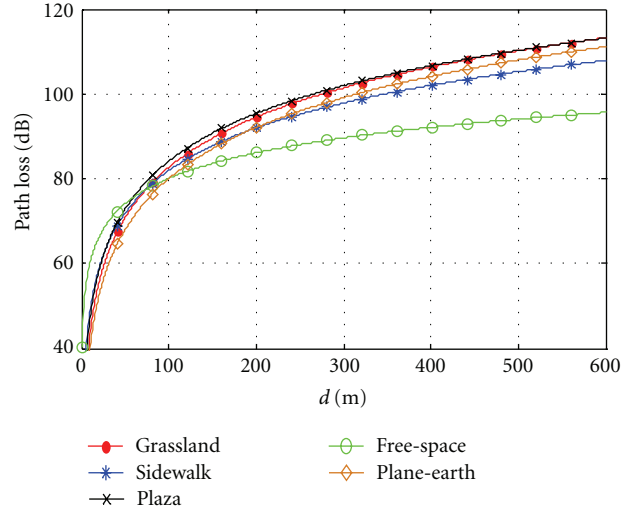
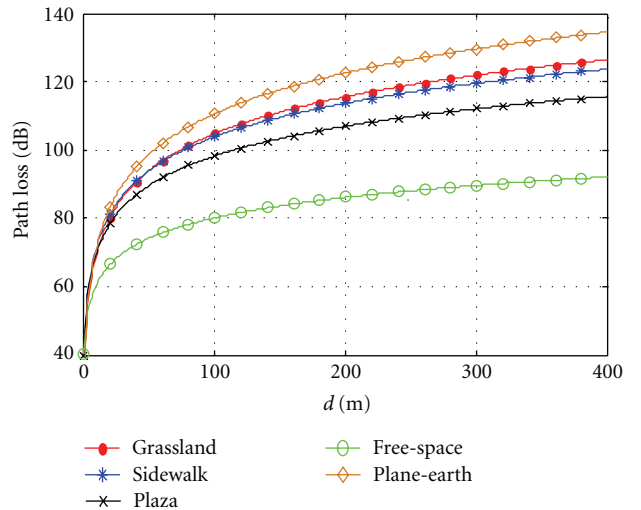
When the radio wave propagates near the ground with a line-of-sight (LOS) condition, the path loss can be better described by the plane-earth (PE) path loss model rather than the free-space model [10]. The plane-earth path loss model [19] includes antenna heights and the effect of ground reflection, which is given as

$$L_{PE} = 40 \log_{10}(d) - 20 \log_{10}(h_t) - 20 \log_{10}(h_r), \quad (8)$$

where d is the distance between the transmitter and receiver in meters; h_t and h_r are the transmitting and receiving antenna heights in meters, respectively. It is necessary that d be much larger than the h_t and h_r when using the model.

The path loss predicted by the two-slope model is plotted in Figures 6–8, together with those predicted by the free-space model and the plane-earth model. Since the prediction of the path loss in far field is the main concern, only the second segment of the two-slope model is used.

From Figure 6, it is found that the values predicted by the plane-earth model are close to the values predicted by the proposed model, and the difference at 600 m is by 2.1–3.2 dB. This is because the LOS conditions are present in the three sites when both the antenna heights are set to 1 meter, where the two-ray propagation mechanism is dominant. Since the optimization of the plane-earth model is based on the two-ray propagation mechanism [19], its high prediction accuracy is expected. As the transmitting antenna height decreases, the ability of the plane-earth model to predict the path loss becomes poor. As can be seen from Figures 7 and 8, the plane-earth model overestimates the path loss significantly by 8–18.8 dB more than the value predicted by the proposed model at 400 m. This is mainly due to the disappearance of the LOS conditions when the transmitting antenna height is lowered, and other propagation mechanisms are not taken into account by the plane-earth model, such as the forward scattering mechanism

FIGURE 6: Comparisons between the proposed model and the generic model ($h_t = h_r = 1$ m).FIGURE 7: Comparisons between the proposed model and the generic model ($h_t = 3$ cm, $h_r = 1$ m).

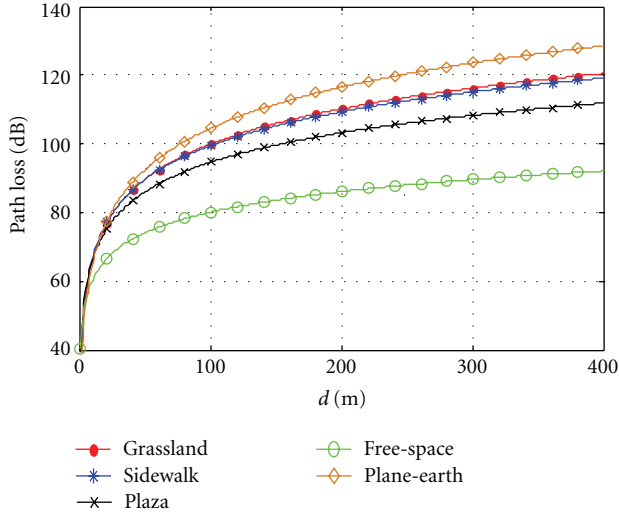


FIGURE 8: Comparisons between the proposed model and the generic model ($h_t = 3$ cm, $h_r = 2$ m).

mentioned in Section 4.1. On the contrary, the free-space model underestimates the path loss dramatically by 19.8–34.3 dB at 400 m, which further indicates that the near-ground channel is far from a free space.

The unfitness of these two generic models can be further verified by the d_{\max} values in Table 1. It is obvious that the d_{\max} value for the plane-earth model is far less than for the proposed model at the same antenna height, while the value for the free-space model is much larger than that of the proposed model. Therefore, it can be concluded that, for the near-ground scenarios, the two generic models will lead to large errors for the path loss prediction, which makes them unfeasible.

5. Conclusions

This paper performs experimental path loss modeling for three near-ground sites at 2.4 GHz frequency. The linear regression based on the measured data indicates that the log-distance-based model is still suitable for path loss modeling in near-ground sites, and the prediction accuracy of the two-slope model is higher than that of the one-slope model. The obtained path loss exponent is less than 2 before the breakpoint and then between 2 and 4, which is in accordance with the results in [17]. The breakpoint distance is mainly determined by the antenna height with slight environmental influences, which is contrary to the conclusions in [3]. For the sidewalk and the grassland sites, an increase of 4.31–5.9 dB in the path loss is observed as the receiving antenna height decreases from 2 to 1 m, which roughly accords with the rule that the path loss increases by 6 dB as the antenna height is halved. However, in cases of much lower antenna height, the path loss increases by 20.1–21.97 dB as the transmitting antenna height decreases from 1 m to 3 cm, suggesting that this rule is not applicable. The proposed model for each site is well matched with the authentic channel environment, which is further verified by the comparisons

between the predicted path loss and the measured path loss in far field. Comparisons between the proposed model and the generic models indicate that the near-ground channel (with flat terrain) is far from a free space, and the free-space model will lead to large errors for the path loss prediction. Although the plane-earth model takes the effect of antenna height into consideration, its ability to accurately predict the path loss is still poor. To achieve higher prediction accuracy, the path loss modeling based on the measured data is very necessary. The results presented here can thus be referred for the design and performance simulation of WSN systems in near-ground scenarios.

Acknowledgment

This work was partly supported by the Foundation of National Key Laboratory for Electronic Measurement Technology, China (2011YF003).

References

- [1] C. Fitzhugh, J. Frolik, R. Ketcham, J. Covell, and T. Meyer, "Multipath fading in airframes at 2.4 GHz," in *Proceedings of the IEEE Annual Conference on Wireless and Microwave Technology (WAMICON '05)*, pp. 162–165, Clearwater, Fla, USA, April 2005.
- [2] A. Fanimokun and J. Frolik, "Effects of natural propagation environments on wireless sensor network coverage area," in *Proceedings of the 35th Southeastern Symposium on System Theory*, pp. 16–20, Morgantown, WV, USA, March 2003.
- [3] A. Martínez-Sala, J. M. Molina-García-Pardo, E. Egea-López, J. Vales-Alonso, L. Juan-Llaser, and J. García-Haro, "An accurate radio channel model for wireless sensor networks simulation," *Journal of Communications and Networks*, vol. 7, no. 4, pp. 401–406, 2005.
- [4] A. Hugine, H. I. Volos, J. Gaedert, and R. M. Buehrer, "Measurement and characterization of the near-ground indoor ultra wideband channel," in *Proceedings of the IEEE Wireless Communications and Networking Conference (WCNC '06)*, pp. 1062–1067, Las Vegas, Nev, USA, April 2006.
- [5] J. Karedal, S. Wyne, P. Almers, F. Tufvesson, and A. F. Molisch, "A measurement-based statistical model for industrial ultra-wideband channels," *IEEE Transactions on Wireless Communications*, vol. 6, no. 8, pp. 3028–3037, 2007.
- [6] K. Phaebua, C. Phongcharoenpanich, D. Torrungrueng, and J. Chinrungrueng, "Short-distance and near-ground signal measurements in a car park of wireless sensor network system at 433 MHz," in *Proceedings of the 5th International Conference on Electrical Engineering/Electronics, Computer, Telecommunications and Information Technology (ECTI-CON '08)*, pp. 241–244, Krabi, Thailand, May 2008.
- [7] K. Sohrabi, B. Manriquez, and G. J. Pottie, "Near ground wide-band channel measurement in 800-1000 MHz," in *Proceedings of the IEEE VTS 50th Vehicular Technology Conference (VTC '99)*, pp. 571–575, Houston, Tex, USA, September 1999.
- [8] R. A. Foran, T. B. Welch, and M. J. Walker, "Very near ground radio frequency propagation measurements and analysis for military applications," in *Proceedings of the IEEE Military Communications Conference (MILCOM '99)*, pp. 336–340, Atlantic City, NJ, USA, November 1999.
- [9] T. B. Welch, J. N. Wood, R. W. I. McFarlin et al., "Very near ground RF propagation measurements for wireless systems,"

- in *Proceedings of the 51st Vehicular Technology Conference (VTC '00)*, pp. 2556–2558, Tokyo, Japan, May 2000.
- [10] G. G. Joshi, C. B. Dietrich Jr., C. R. Anderson et al., “Near-ground channel measurements over line-of-sight and forested paths,” *IEEE Proceedings*, vol. 152, no. 6, pp. 589–596, 2005.
 - [11] Y. S. Meng, Y. H. Lee, and B. C. Ng, “Near ground channel characterization and modeling for a tropical forested path,” 2011, <http://www.ursi.org/proceedings/procGA08/papers/FP1p10.pdf>.
 - [12] R. Urban and S. Zvánovec, “Dispersion and pulse interferences investigation for UWB signal propagation,” *Radioengineering*, vol. 17, no. 3, pp. 60–65, 2008.
 - [13] J. C. R. Dal Bello, G. L. Siqueira, and H. L. Bertoni, “Theoretical analysis and measurement results of vegetation effects on path loss for mobile cellular communication systems,” *IEEE Transactions on Vehicular Technology*, vol. 49, no. 4, pp. 1285–1293, 2000.
 - [14] R. Akl, D. Tummala, and X. Li, “Indoor propagation modeling at 2.4 GHz for IEEE 802.11 networks,” 2011, <http://www.cse.unt.edu/~rakl/ATL06.pdf>.
 - [15] T. S. Rappaport, *Wireless Communications: Principles and Practice*, Prentice Hall, New York, NY, USA, 2nd edition, 2001.
 - [16] A. Goldsmith, *Wireless Communications*, Cambridge University Press, Cambridge, UK, 2005.
 - [17] H. H. Xia, H. L. Bertoni, L. R. Maciel, A. Lindsay-Stewart, and R. Rowe, “Radio propagation characteristics for line-of-sight microcellular and personal communications,” *IEEE Transactions on Antennas and Propagation*, vol. 41, no. 10, pp. 1439–1446, 1993.
 - [18] J. Lavergnat and M. Sylvain, *Radio-Wave Propagation: Principles and Technique*, Wiley, New York, NY, USA, 2000.
 - [19] J. D. Parsons, *The Mobile Radio Propagation Channel*, Wiley, New York, NY, USA, 2nd edition, 2000.

